

The effect of stacking fault energy on the microstructural development during room temperature wire drawing in Cu, Al and their dilute alloys

S. K. VARMA, V. CABALLERO, J. PONCE, A. De La CRUZ, D. SALAS
Department of Metallurgical and Materials Engineering, The University of Texas at El Paso, El Paso, TX 79968-0520, USA

The effect of stacking fault energy (SFE) on the evolution of microstructures during wire drawing at room temperature has been studied in pure aluminium, pure copper and Cu–2.2% Al and Cu–4.5% Al alloys which covers a range of SFE values from 4 to 166 mJ m⁻². The compositions are expressed in atomic parts per million by weight. The microstructures have been characterized from samples obtained by deforming rods of these materials to true wire drawing strain values of up to 1.47. A decrease in the SFE value changes the deformation mechanisms from the formation of cell structure and their size refinement in a high SFE material to the formation of deformation bands and deformation twins in a low SFE materials. The Cu–2.2% Al alloy deforms by deformation bands at low true strain values while deformation twins within the bands control the deformation mechanisms at higher true strain values. The alloy, Cu–4.5% Al, with the lowest SFE value deforms only by deformation twins even at low true strain values and the presence of overlapping and intersecting deformation twins are the dominating features as the rods are drawn to higher true wire drawing strains.

1. Introduction

The major influence of stacking fault energy (SFE) on the microstructures produced during deformation is through the dynamic recovery. The extent of dynamic recovery in high SFE materials is large with the result that the dislocations can easily cross slip and the formation of cell structure in the early stages of deformation is inevitable. Further strain during the deformation is accommodated by the material in the form of cell wall sharpening, cell size decrease, increase in misorientation angle between the cells and eventually dynamic recrystallization can result (in this particular sequence) under favourable conditions. On the other hand, limited dynamic recovery in low SFE materials can restrict the dislocation motion to only planar slip. Large amounts of deformation in low SFE materials can be accommodated through the formation of deformation bands, microbands and most importantly deformation twins. Thus the change in mechanism for the deformation from the formation of cell structure and cell size refinement to deformation twins can be considered as the two extremes to be expected when a complete spectrum of SFE values are considered.

The SFE values for copper and aluminium are 78 and 166 mJ m⁻² respectively [1]. The effect of SFE on the development of microstructures in these two metals during room temperature wire drawing process indicates the following features as the basis for

comparison: (a) the formation of well defined cell structure appears at lower true strains in aluminium [2], (b) the cell size is smaller at equivalent true wire drawing strains in copper [2, 3] and (c) there is definite evidence of dynamic recrystallization in aluminium for true strain values as low as one [4]. No evidence of twin formation during the wire drawing of copper has been reported in the literature even though the SFE value is slightly less than half of the SFE value for aluminium. Thus the wire drawing deformation does not show any change in deformation mechanism for two metals that differ in their SFE values by more than half. However, a change in deformation mechanism may be expected for values of SFE less than 78 mJ m⁻². Thus the purpose of this study was to perform similar deformation (wire drawing) for two alloys of copper and aluminium, Cu–2.2% Al and Cu–4.5% Al, whose SFE values are 20 and 4 mJ m⁻² respectively [1], and compare the deformation mechanism with the two metals in their pure forms.

2. Experimental procedure

Four nines purity (Table I) copper and aluminium was used in this study and the same pure metals were mixed to obtain the alloys, Cu–2.2% Al and Cu–4.5% Al (compositions have been expressed in atomic parts per million by weight throughout this

TABLE I Chemical composition of copper in atomic parts per million by weight

Bi	Pb	O	P	Se	S	Te	Cu
10	10	5	3	10	15	10	Bal.

Chemical composition of aluminium in atomic parts per million by weight

O	Cu	Fe	B	Ni	Si	C	Al
23	20	7	5	4	4	3	Bal.

paper). Copper rods of 9.525 mm diameter and six foot in length were annealed for 2 h at 450 °C in an inert argon gas atmosphere. The diameter of the annealed rods were reduced to finer wires by room temperature wire drawing through a set of dies of the following sizes: 9.246 (0.364"), 8.23 (0.324"), 7.341 (0.289"), 6.528 (0.257"), 5.817 (0.229"), 5.182 (0.204") and 4.597 (0.181") mm. The chosen dies provide for a standard reduction of 13% in cross-sectional area per pass. It was possible to get 40 feet lengths of five different wires, in addition to the initial 9.525 mm diameter rod, of 8.23, 7.341, 6.528, 5.817 and 4.597 mm diameter corresponding to true wire drawing strains of 0.29, 0.52, 0.76, 0.99 and 1.47 respectively.

The pure aluminium was melted in an induction heating unit using a graphite crucible under an inert atmosphere of ultra high purity (UHP) argon gas. This was performed by outgassing the casting system with a mechanical pump and then back filling the system with UHP argon gas for the melting. A 101.6 mm (4") ingot was extruded at 350 °C to obtain a 25.4 mm diameter rod at room temperature which was further reduced to a rod diameter of 9.525 mm by swaging. This rod was then annealed at 450 °C for two hours to obtain a starting material for the final wire drawing operation as described above in this section.

The alloys were fabricated by melting the pure metals in an induction heating unit. The melting procedure for the alloys was similar to those described for aluminium in the previous paragraph. The temperature of the molten liquid was held at a super heat of 150 °C and the casting was performed to obtain an ingot of 101.6 mm in diameter. The alloys were then used to produce five different diameter wires through a procedure identical to that described for pure aluminium in this section.

The transmission electron microscopy (TEM) sample preparation technique involved the cutting of a wafer of 0.5 mm thickness from the short cross-section of the wires with the help of Buehler Isomet slow cutting machine. Samples of 0.3 mm diameter were punched out of this wafer after it had been hand ground to a thickness of 0.2 mm. The discs were then electropolished in a twin jet Struer's Tenupol 3 electropolishing machine. The details of electropolishing conditions can be seen in Table II. The TEM observations were performed using a Hitachi H-8000 scanning transmission electron microscope (STEM) operating at an accelerating voltage of 200 kV. At least four different foils were examined for each wire at magnifications ranging from 7500–30 000.

TABLE II Electropolishing conditions for the materials used in this study

Material	Electrolyte composition	Temp (°C)	Volts (V)	Flow rate
Al	Nitric Acid, 1 part Methanol, 3 parts	– 20	13	9
Cu	Distilled Water, 1100 ml Phosphoric Acid, 400 ml Ethanol, 500 ml Propanol, 100 ml Urea, 10 g	10	10	10
Cu–2.2% Al	Same as Cu	– 1	15	10
Cu–4.5% Al	Same as Cu	5	30	7

3. Results and discussion

The characterization of the microstructures created by room temperature wire drawing of pure aluminium, pure copper, Cu–2.2% Al and Cu–4.5% Al alloys with SFE values of 166, 78, 20 and 4 mJ m^{–2}, respectively, will be discussed in the descending order of SFE values.

3.1. Pure aluminium

The TEM micrographs of the deformed wires indicate the presence of dislocation cells in the microstructure as is shown in Fig. 1. At a strain of 0.29, the cell walls initially appear to be quite thick as is shown in Fig. 1a which is an indication of a rather low dislocation density in the wire. The formation of a cell structure in high SFE metals has been explained on the basis of a reduction in overall energy created by the rearrangement of dislocations from their existing distribution into cellular form [5–7]. The deformation increases the total dislocation density and the microstructure absorbs the additional dislocations within the cell boundaries making them somewhat sharper [8–11]. The increase in dislocation density results in a decrease in the cell size according to those theories of dislocation cell structures [12, 13] that are supported with experimental evidence [14]. The decrease in cell size can also be accompanied by an increase in the misorientation angle between the cell walls [15, 16].

Fig. 1 shows that once a cell structure develops the increase in dislocation density is manifested in cell wall sharpening in addition to the cell size decrease. The cell size changes during deformation in pure aluminium appear to be different in different studies varying from reaching a cell size saturation [2] to an alternate increase and decrease in the size at higher strain values [4]. Even though the cell sizes were not measured in this study it can be qualitatively interpreted that the cell size decreases up to a true wire drawing strain of 1.47 without any evidence of dynamic recrystallization during the process. We believe that any unusual behaviour of the cell size variation with strain, as reported by several authors in the literature, may be an artifact of the purity of the aluminium, the type of deformation, the strain rate and also to a certain extent, the initial grain size [9, 10].

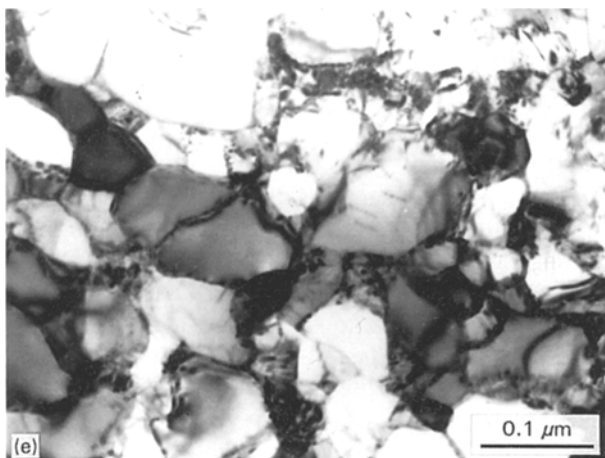
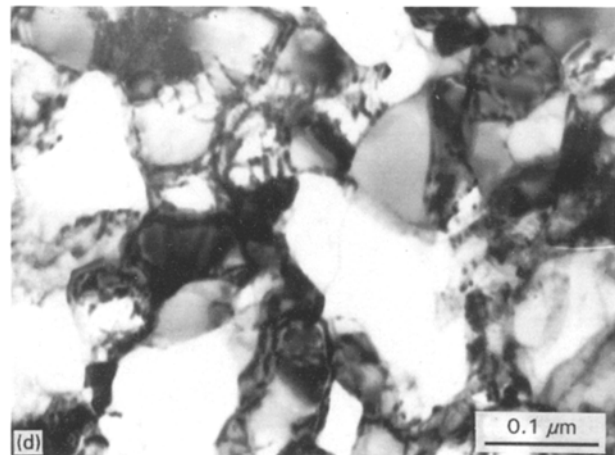
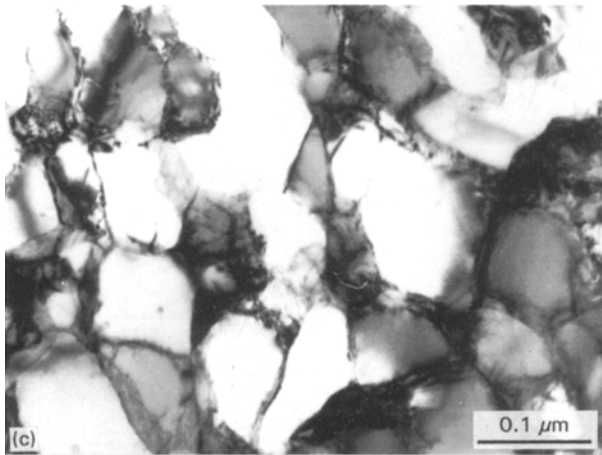
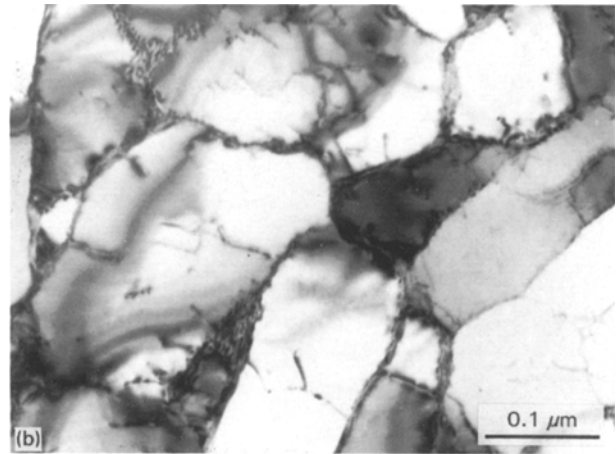
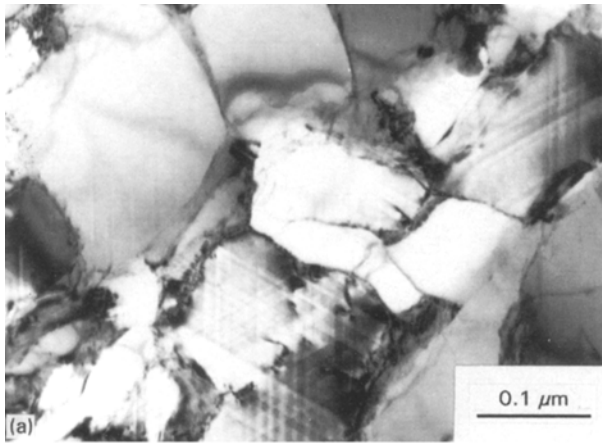


Figure 1 The TEM micrographs of the short cross-sections of pure aluminium wires drawn to true wire drawing strain of (a) 0.29, (b) 0.52, (c) 0.76, (d) 0.99, and (e) 1.47.

3.2. Pure copper

The TEM micrographs of the copper wires indicate the formation of a cell structure at a strain of 0.29 as is shown in Fig. 2a. A striking feature appears to be the difference in cell sizes as shown in Figs 1 and 2. The cell sizes observed in copper are smaller than those observed in pure aluminium at similar strains, a feature that can be attributed to the lower SFE value of copper. The dislocations within the cell walls appear not to be as efficiently packed with dislocations as they were in the case of aluminium since the cell boundaries in Fig. 2 are not very sharp. It must be noted that no attempt has been made to quantify the microstructural features observed in this study

since the objective of this study was to qualitatively understand the microstructural development taking place during the selected deformation process as a result of the changes in the SFE values of the metals and alloys.

3.3. Cu–2.2% Al alloy

The TEM micrographs of the short cross-sections of the wires of the Cu–2.2% Al alloy are shown in Fig. 3. The presence of a large number of deformation bands in the microstructure at a strain of 0.29 can be seen in Fig. 3a. It must be noted that an attempt was made to determine the misorientation angle between the band and the matrix in this study. It was observed that no measurable differences in the orientation between the two could be detected. Hung and Gray [17], however, have reported that microbands are typically misoriented with the matrix by a range of angles from 1–3°. The typical widths, 0.1–0.5 μm, of the bands, observed in this study, appear to be in a range of values for the microbands reported by these authors.

The bands contain the substructure, in the form of a nonuniform distribution of dislocations at low true wire drawing strain values. However, as the strain increases not only does the number of deformation

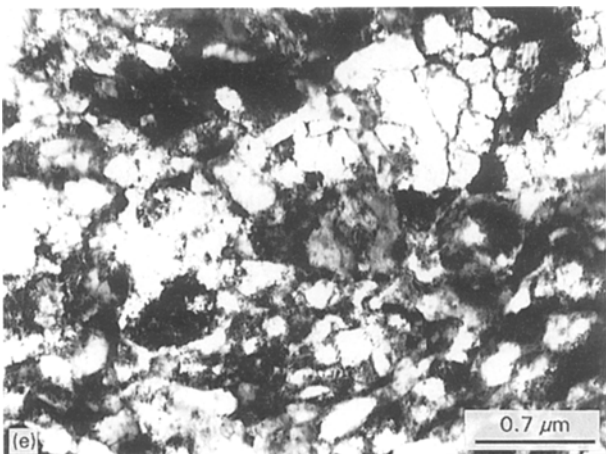
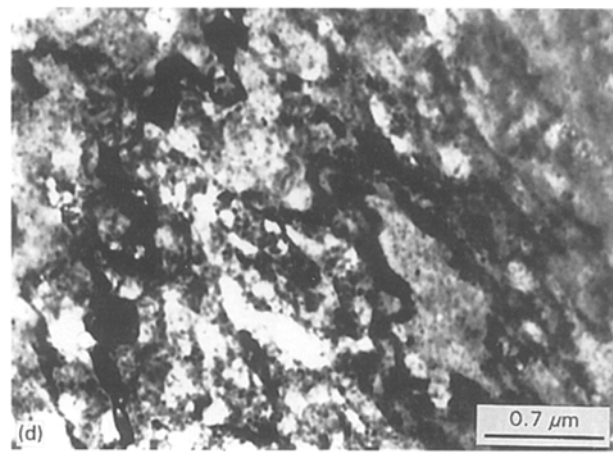
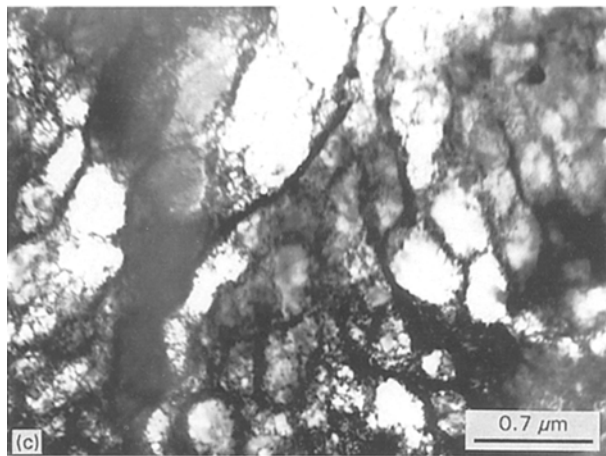
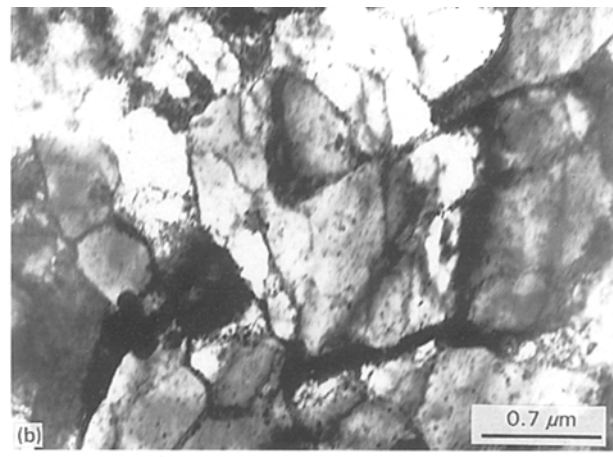
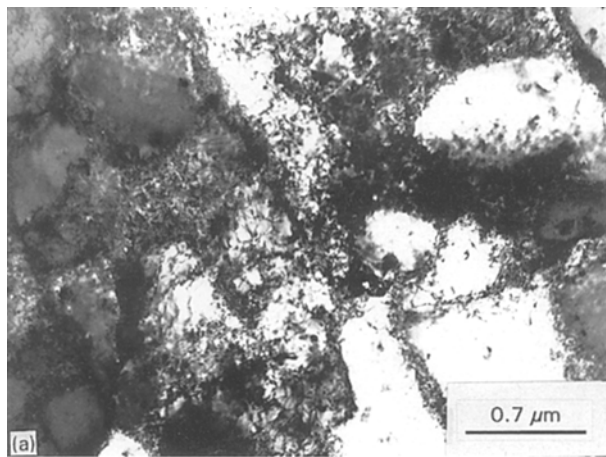


Figure 2 The TEM micrographs of the short cross-sections of pure copper wires drawn to true wire drawing strain of (a) 0.29, (b) 0.52, (c) 0.76, (d) 0.99, and (e) 1.47.

bands increase but also the internal substructure also appears to change from a non uniform distribution of dislocations to a deformation twin structure. The deformation at higher strains must then be confined to the bands and takes place through the deformation twins. The density of bands as well as that of the deformation twins increases with an increase in the strain indicating that the alloy deforms by deformation bands containing deformation twins. The overlapping of deformation bands has also been observed in the microstructure, Fig. 3d, which can be an indication of the accommodation of strain in the microstructures by slip planes generated from (111) planes.

The bands have been considered to be overlapping and not intersecting because there is no indication of the offset that would be present if the two bands were intersecting each other. The extent of offset would be an indication of the amount of strain absorbed in the material [18, 19]. The dominant directions of the bands run mostly in the [112] and [110] directions on the (111) planes which was established from diffraction patterns taken on several samples of this alloy.

The presence of the deformation twins has been confirmed by selected area diffraction patterns. Fig. 4a shows a bright field image of a sample of this alloy and Fig. 4b is the diffraction pattern from the area we believe contains deformation twins. The dark field image corresponding to a spot formed by the twin is shown in Fig. 4c. It can be seen in Fig. 4c that there is a definite reversal of the contrast in comparison to its corresponding bright field image shown in Fig. 4a. We thus conclude that the deformation bands deform preferentially by deformation twins compared to the deformation of the rest of the matrix which must then deform with greater difficulty. The matrix does not delineate any definite pattern of dislocation cell structure.

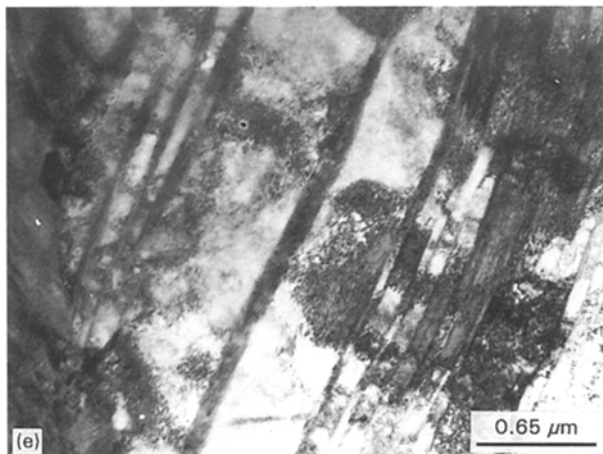
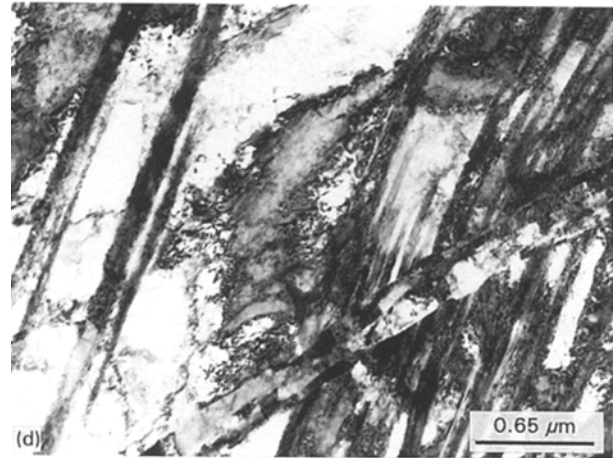
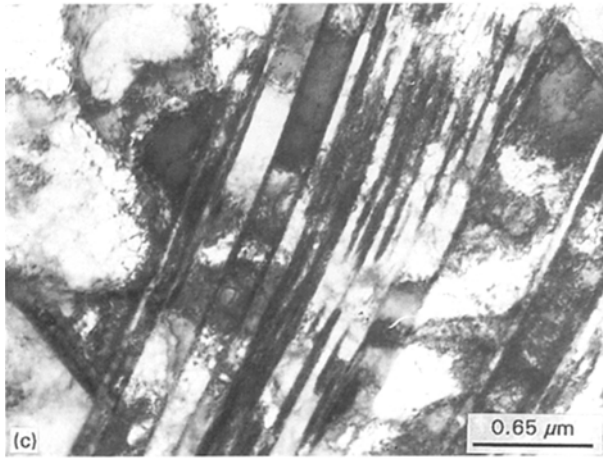
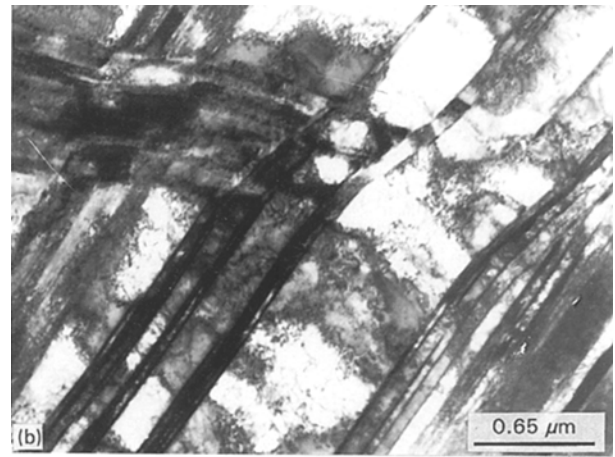
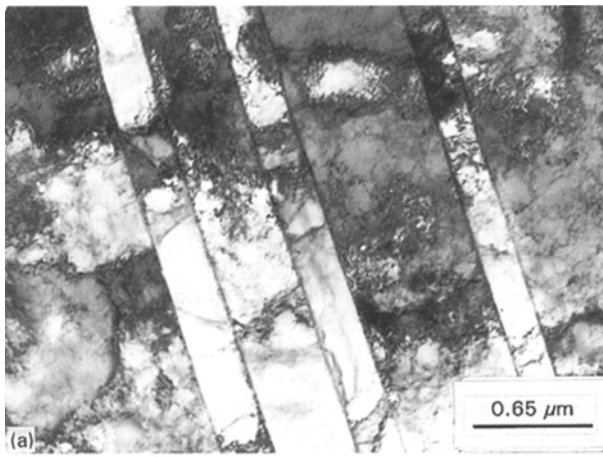


Figure 3 The TEM micrographs of the short cross-sections of the wires of Cu-2.2% Al alloy drawn to true wire drawing strain of (a) 0.29, (b) 0.52, (c) 0.76, (d) 0.99, and (e) 1.47.

3.4. Cu-4.5% Al alloy

The TEM micrographs indicate the presence of a large number of deformation twins even at the smallest strain of 0.29 as is shown in Fig. 5a. The twinning direction appears to be [110] in most cases. However, intersecting twins have also been observed in the [112] direction. The number of twins increases with the amount of strain in the alloy and the absence of bands in this case indicates that the primary deformation mode for this alloy with an extremely low SFE value is solely twinning. The twin density increases during the deformation as is shown in Fig. 5. The

figure also reveals that many overlapping twins can be observed in this alloy. Not only is the density of such twins much higher in this alloy compared to the Cu-2.2% Al alloy but also intersecting twins have been observed. Once again the presence of deformation twins has been confirmed by both selected area diffraction patterns and dark field imaging as is shown in Fig. 6(b and c) respectively.

4. Discussion

This study has used two groups of FCC metals and alloys as classified by Hong and Laird: (a) wavy slip materials such as aluminium and copper and (b) planar slip materials such as the two alloys used in this research [20]. The wavy character of the pure metals used in this study apparently follows the typical (tangles and then cell structure formation) microstructural developments expected of high SFE metals. We believe that the SFE effect is not the only material characteristic that should influence the microstructures. The strain rate and initial grain size effects should also be considered as being important.

It has been proposed in the literature [21,22] that the critical composition in the Cu-Al system for the deformation characteristic to change from wavy to

planar slip is around 6 at % Al (the compositions in our present study correspond to 5 and 10 at % Al) in Cu. However, we do not find any evidence for planar slip in our Cu-2.2% Al (equivalent to Cu-5 at % Al) alloy whilst Feltner and Laird [23] report its existence in Cu-7 at % Al alloy in fatigue. The suggestion by Hong and Laird [20] that the transition from fine to coarse slip appearance occurs at 2-3 at % ahead of the transition from wavy to planar dislocation also does not appear to follow the trends of this study. The

presence of deformation twins within the bands in our two alloys indicate that the transition may instead be affected by the change in deformation mechanism from slip to twinning. The microstructures contain mostly deformation twins, with only isolated examples of slip bands, in the Cu-4.5% Al alloy whilst the slip bands contain deformation twins for the Cu-2.2% Al alloy which suggests that at the critical concentration of solute atoms in copper, a direct slip to twin transition mechanism occurs under our experimental

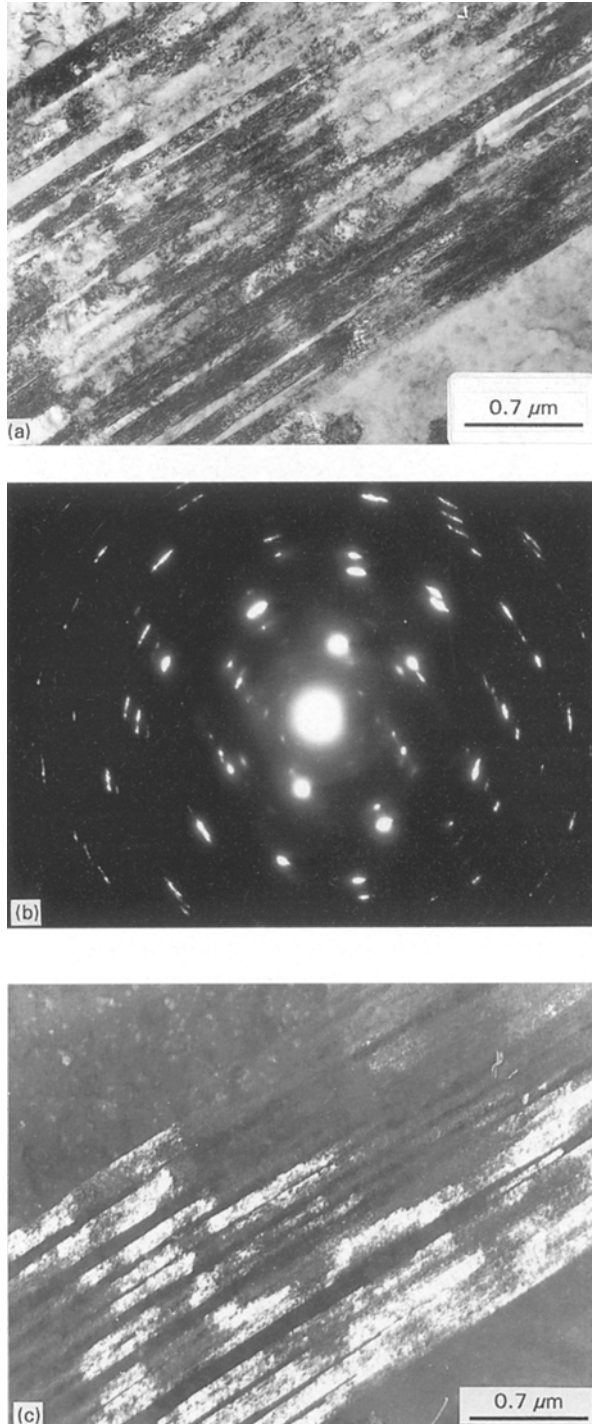


Figure 4 The (a) bright-field image, (b) diffraction pattern from an area containing the bands and the deformation twins within them and (c) the dark field image from a spot in the diffraction pattern corresponding to the twins for a Cu-2.2% Al alloy sample deformed to a true wire drawing strain of 0.99.

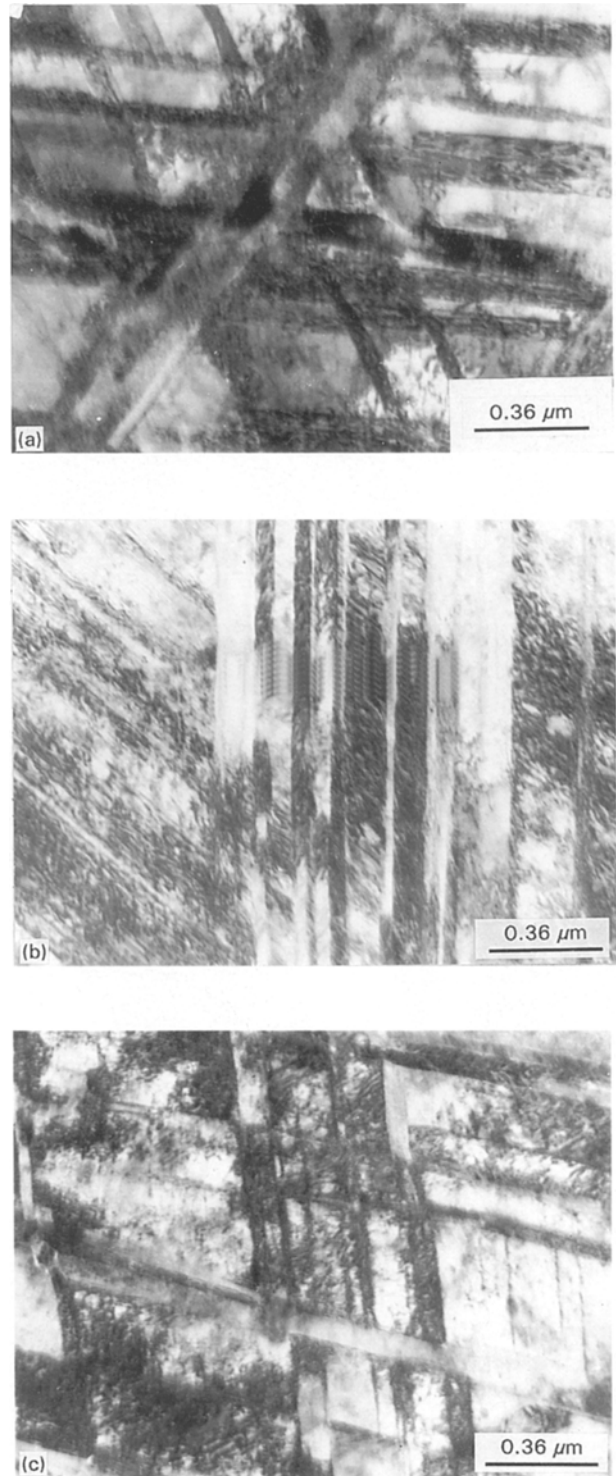


Figure 5 The TEM micrographs of the short cross-sections of the wires of Cu-4.5% Al alloy drawn to true wire drawing strain of (a) 0.29, (b) 0.52, (c) 0.76, (d) 0.99, and (e) 1.47.

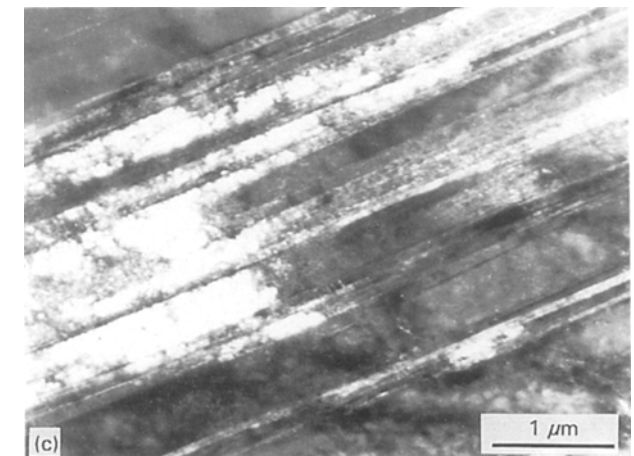
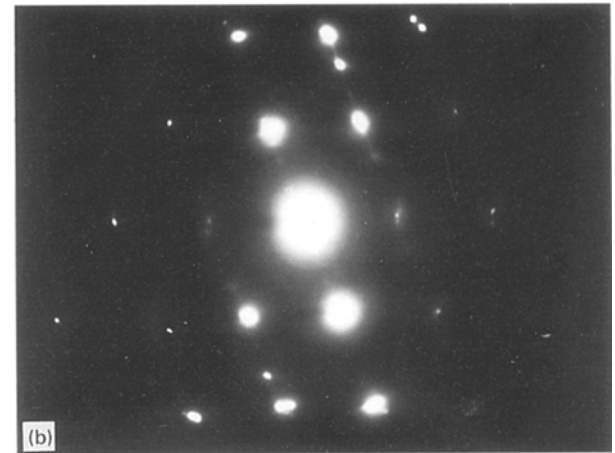
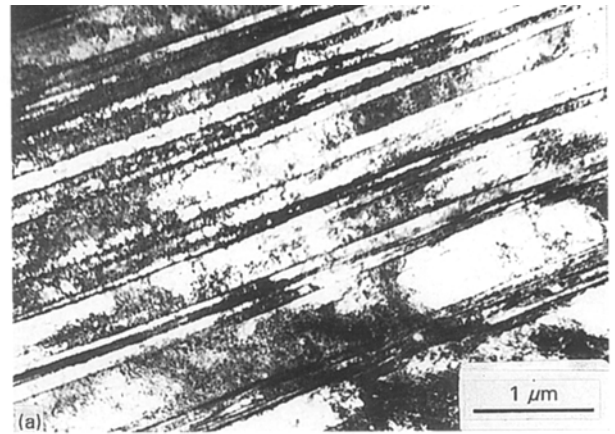
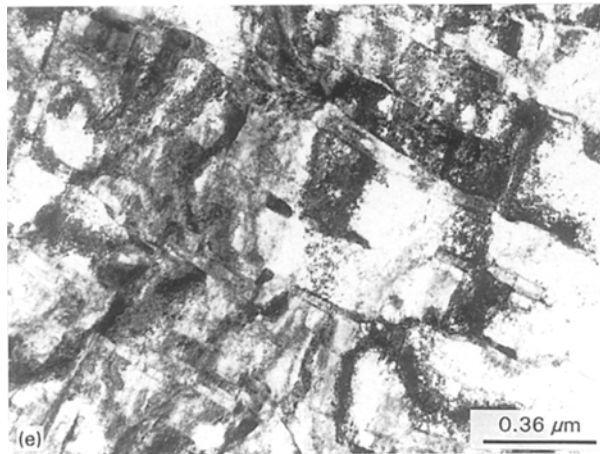
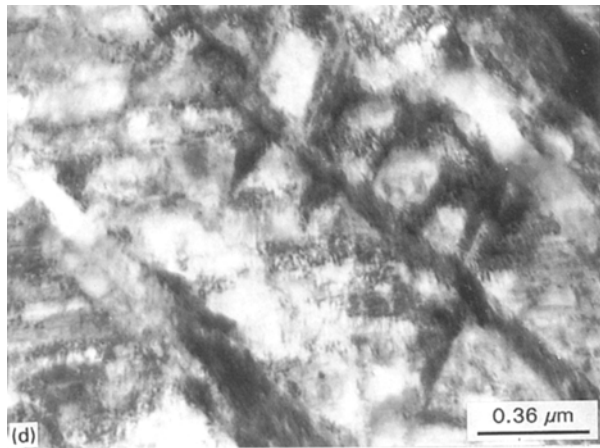


Figure 5 (Continued).

conditions. The results of this study are also in agreement with the fact that deformation by twinning is preceded by a certain amount of slip.

It must be noted that the slip mode is not only affected by changes in the SFE values produced as a result of the addition of solute atoms in the copper but it may also be affected by frictional stress effects [24–26], geometrical effects of the stacking fault [20] and dislocation clustering [20].

5. Conclusions

1. The deformation mechanism by which the aluminium metal with a SFE of 166 mJ m^{-2} deforms has been shown to be initially through the formation of dislocation cell structures with diffuse boundaries. The boundaries become sharper and finally a high dislocation density generated during the wire drawing deformation is accommodated in the microstructures through the decrease in cell size.

2. Copper metal with a SFE of 78 mJ m^{-2} was also investigated in this study. The dislocation cell formation and the cell size refinement during the deformation is a similar microstructural behaviour to that observed in aluminium. However, the cell sizes are smaller in copper than in aluminium under similar processing and strain conditions.

3. Lowering of the SFE to 20 mJ m^{-2} by adding 2.2% aluminium to copper changes the deformation mechanism from the small cellular structures observed in

Figure 6 The (a) bright-field image, (b) diffraction pattern from an area containing the deformation twins and (c) the dark field image from a spot in the diffraction pattern corresponding to the twins for a Cu–4.5% Al alloy sample deformed to a true wire drawing strain of 0.76.

aluminium and copper to an extremely large number of bands in this alloy. The bands further deform by deformation twins.

4. The Cu–4.5% Al alloy, with a SFE value of 4 mJ m^{-2} , deforms mainly by deformation twins and the density of twins increases with an increase in strain during the deformation. The overlapping twins of at least two different orientations, $[110]$ and $[112]$, have been identified in this alloy especially at high strain values.

Acknowledgements

The authors would like to acknowledge the financial support of the National Science Foundation through the research grant number HRD-9353547. Mr Juan Sanchez, a graduate student in our department, provided very useful experimental help in the TEM sample preparation.

References

1. L. E. MURR, "Interfacial Phenomenon in Metals and Alloys", Reprinted by Techbooks (original publisher was Addison-Wesley Publishing Co. Herndon, VA, 1975) pp. 145-148.
2. S. K. VARMA and B. G. LEFEVRE, *Metall. Trans. A* **11A** (1977) 935.
3. J. D. EMBURY, A. S. KEH and R. M. FISHER, *Trans. TMS-AIME* **236** (1966) 640.
4. I. SAMAJDAR and S. K. VARMA, *Mat. Sci. Engng* **A143** (1991) L1.
5. A. W. THOMPSON, *Metall. Trans. A* **8A** (1977) 833.
6. N. HANSEN and D. KUHLMANN-WILSDORF, *Mater. Sci. Engng* **81** (1986) 141.
7. N. HANSEN, *Mater. Sci. Tech.* **6** (1990) 1039.
8. J. J. GRACIO, J. V. FERNANDEZ and J. H. SCHMITT, *Mater. Sci. Engng* **A118** (1989) 97.
9. D. SIL, J. G. RAO and S. K. VARMA, *Metall. Trans. A* **23A** (1992) 3166.
10. D. SIL and S. K. VARMA, *ibid.* **23A** (1993) 1153.
11. J. G. RAO and S. K. VARMA, *ibid.* **24A** (1993) 2559.
12. D. KUHLMANN-WILSDORF, *Mater. Sci. Engng* **A113** (1989) 1.
13. D. L. HOLT, *J. Appl. Phys.* **41** (1970) 3197.
14. M. R. STAKER and HOLT, *Acta Metall.* **20** (1972) 569.
15. G. LANGFORD and M. COHEN, *Metall. Trans. A* **6A** (1975) 901.
16. W. H. ZIMMER, S. S. HECKER, D. L. ROHR and L. E. MURR, *Met. Sci.* **17** (1983) 198.
17. J. C. HUANG and G. T. GRAY III, *Acta Metall.* **12** (1989) 3335.
18. G. T. GRAY III, *J. de Physique IV* **4** (1994) C8-373.
19. *Idem*, in "Twinning in Advanced Materials", edited by M. H. Yoo and M. Wuttig (The Minerals, Metals and Materials Society, Pittsburg, PA, 1994) pp. 337-349.
20. S. I. HONG and C. LAIRD, *Acta Metall.* **38** (1990) 1581.
21. P. J. WOODS, *Phil. Mag.* **28** (1973) 155.
22. H. MORI and H. FUJITA, *J. Phys. Soc. Jpn* **38** (1975) 1342.
23. C. E. FELTNER and C. LAIRD, *Acta Metall.* **15** (1967) 1633.
24. U. F. KOCKS, *Metall. Trans. A* **16A** (1985) 2109.
25. H. NEUHAUSER, O. B. ARKAN and H. H. POTTHOFF, *Mater. Sci. Engng* **81** (1986) 201.
26. U. F. KOCKS, R. E. COOK and R. A. MULFORD, *Acta Metall.* **33** (1985) 623.

Received 7 September 1995
and accepted 15 January 1996